

Perturbation Theory on the Transition Temperature and Electronic Properties of Organic Superconductor

Takanobu JUJO*, Shigeru KOIKEGAMI and Kosaku YAMADA

Department of Physics, Kyoto University, Kyoto 606-8502

(Received to be published in JPSJ (1999) No. 4)

We study the superconducting transition temperature and the electronic properties of the metallic phase of κ -type (BEDT-TTF)₂X which shows unconventional properties in experiments, on the basis of the third order perturbation theory for a simple effective Hubbard model of a nearly triangular lattice. Appropriate transition temperatures and $d_{x^2-y^2}$ symmetry of the gap function are obtained in good agreement with experimental results. We also calculate the transition temperature by the fluctuation-exchange approximation(FLEX) in order to compare the two approaches; FLEX gives higher transition temperatures rather than the perturbation approach. However, it is also found that the vertex corrections, which are ignored in FLEX, have a crucial effect on T_c for strongly frustrated systems. The density of states and the normal self-energy calculated in this perturbation scheme show the nature of the conventional Fermi liquid near the Mott-insulator. Thus, our perturbation approach is applicable to the conventional metallic phase of this compound, while it cannot explain the (pseudo-)spin gap phenomenon which signals the non-Fermi liquid.

KEYWORDS: perturbation approach, electron correlation, spin fluctuation, vertex correction, Fermi liquid, d-wave superconductor, density of states, self-energy

§1. Introduction

Today, there are many organic compounds which show the superconductivity at low temperatures. One of the most interesting superconductors among these compounds is κ -type (BEDT-TTF)₂X (X=Cu(NCS)₂, Cu[N(CN)₂]Br, Cu[N(CN)₂]Cl and κ -(ET)₂X for an abbreviation). These compounds show superconductivity under the pressure appropriate to each compound. We have two ordered phases by varying pressure, one of which is antiferromagnetic insulator in the lower pressure region and the other is superconductivity in the higher pressure region.¹⁾

By the nuclear magnetic resonance(NMR) experiments, it has been confirmed that, below the transition temperature(T_c), there are no coherence peaks, the Knight shifts decrease and the spin lattice relaxation rate behaves as T^3 .²⁾ These results imply that the symmetry of the Cooper pair is not the isotropic s-wave, but the anisotropic symmetry and spin singlet, indicating the d-wave. These properties are quite similar to the cuprate superconductors (high- T_c). The mechanism of this superconductivity cannot be explained on the basis of the conventional phonon-mediated superconductivity, which usually shows s-wave property and the isotope effect.

Theoretically the unconventional superconductivity have been discussed keeping high- T_c cuprates in mind, roughly speaking from two approaches which are the theory based on the resonating-valence-bond(RVB) state³⁾ (t - J model) and the spin-fluctuation model.^{4),5),6)} In these approaches RVB theory assumes a strong on-site

Coulomb interaction, and is expected to be effective to the doped Mott insulator like the high- T_c materials in the underdoped region. On the other hand, our system is metallic although it has the nature of the half-filling; this fact suggests that the on-site Coulomb interaction is not so strong. Therefore, we consider the weak-coupling approach is appropriate to this superconductor. When we discuss the spin-fluctuation mediated superconductivity, we have several methods of determining the attractive force. Moriya, *et al.* determined $\text{Im}\chi(\mathbf{q},\omega)$ (the imaginary part of the dynamical susceptibility) by the self-consistent renormalization(SCR),⁴⁾ and Pines, *et al.* determined it by NMR experimental results.⁵⁾ They solved the Éliashberg equation by using the phenomenologically determined susceptibility, and obtained the appropriate T_c . Before them, simple calculations by the Random Phase Approximation (RPA) were done by Shimahara *et al.*⁶⁾ However, the T_c obtained by this method was rather lower than those of the above methods owing to the over-estimated damping effect as pointed out by Hotta.⁷⁾ (It should be noted that Shimahara also explored the possibility of spin-fluctuation mediated superconductivity in the organic superconductor (TMTSF)₂X.)

These theories are expected to be effective to κ -(ET)₂X which shows strong antiferromagnetic spin fluctuation as observed by NMR experiments. Here, in order to understand these compounds on the basis of a more microscopic model, we take the following approach.

Because this superconductivity occurs only near the Mott-insulating phase under the controlled pressure, the electron correlation on the same site is expected to play an important role on the appearance of this superconductivity. One of methods to investigate elec-

* E-mail: jujo@ton.scphys.kyoto-u.ac.jp

tron correlation-induced superconductivity is the perturbation method, with respect to Coulomb repulsion U . In the studies of the transition temperature for the high- T_c cuprates, this method was adopted by Hotta.⁷⁾ He calculated T_c by the third order perturbation treatment (TOPT), and discussed the effect of the normal self-energy and the vertex correction on the calculated T_c and then found out that the vertex corrections suppress T_c , compared with that obtained by a summation of the RPA-like diagrams.

Another method of investigating this kind of superconductivity from the weak coupling regime is the fluctuation exchange approximation (FLEX),⁸⁾ which is a kind of the self-consistent calculation based on the RPA-like diagrams. The use of this method is reasonable because the anisotropic superconductivities usually appear near the magnetic ordered phase by controlling the pressure or the doping of carriers. Therefore, the summation of the specific diagrams which are favorable to the spin fluctuation may be justified. However, in this work we concentrate on TOPT, without assuming the strong spin fluctuation like FLEX because it is not clear yet whether taking only the effect of particular diagrams is reliable for revealing the mechanism of superconductivity.

The perturbation approach is sensitive to the dispersion of the bare energy band by its nature, it implies that the lattice structures and the band filling play the essential roles in the calculation of T_c and the electronic properties. Although the TOPT calculation is already performed for the high- T_c , it is important for the study of this compound to calculate T_c newly on the basis of the effective model of κ -(ET)₂X.

In this paper we calculate T_c for the simple effective model by TOPT and investigate its U -dependence and the dependence on the effect of the frustration. Recently the calculations of T_c by FLEX were performed by Schmalian⁹⁾ and Kino *et al.*, Kondo *et al.*¹⁰⁾ on the two-band model and the single-band model respectively. Therefore we also calculate T_c by FLEX because these calculations were performed separately and there is no comparison with other methods yet; it is meaningful to compare the results by TOPT and FLEX. We also estimate the contribution of the vertex corrections, by comparing the results of the full TOPT calculation with that of only RPA-like terms included in anomalous self-energies.

Another prominent property of this compound is the appearance of the (pseudo-)spin gap, which was revealed by the NMR experiments in the metallic phase.¹¹⁾ Therefore, it is necessary to study the electronic properties in order to see what extent our model and approximation which are used to calculate T_c are pertinent to. We calculate the density of states and the normal self-energy, as the physical quantities characterizing the metallic phase of this compound, and then discuss the results and further problems.

§2. Formulation

2.1 Hamiltonian

First we define the effective Hamiltonian in a minimum form which describes κ -(ET)₂X for the calculation of T_c .

The Fermi surface (FS) of κ -(ET)₂X was studied by the Shubnikov-de Haas effect and found that it is well reproduced by the tight binding approximation based on the extended Hückel approximation.¹²⁾ However it is known that a pair of ET molecules is considered as the basic structural unit (which is called a dimer) of the conduction sheet of κ -(ET)₂X because the intradimer hopping term is more than twice of the interdimer one.^{13),14)} Here, we briefly discuss the dimer model, which can be described as Fig. 1.

EPS File fig1.ps not found

Fig. 1. (a) The original lattice structure of κ -(ET)₂X when BEDT-TTF molecules are written explicitly. The line represents each molecule. t_d is the intradimer transfer integral. t_1 , t_2 and t_3 constitute the interdimer transfer integral. (b) The lattice structure of κ -(ET)₂X when the pair of molecules is dimerized. The circle represents a dimer, and the area which are surrounded by dashed lines, represent the unit cell in this case. t and t' are transfer integrals connecting the sites.

The arrangement of BEDT-TTF molecules are shown in Fig. 1 (a). When a dimer is considered as a structural unit, the energy splitting between the bonding and antibonding orbitals is approximately given by $2t_d$. Therefore we can neglect the mixing between the bonding and antibonding orbitals, and the dimer model is verified. Focusing on the antibonding orbital, each dimer is connected to the nearest sites by two kinds of transfer integrals. These transfer integrals can be written as $t = (t_1 + t_2)/2$ and $t' = t_3/2$. (The transfer integrals t_1 , t_2 and t_3 correspond to those of Fig. 1 (a).) Thus, the lattice structure can be described as Fig. 1 (b) by using the above value of t and t' .

Strictly speaking, transfer integrals t in Fig. 1 have two different values which cause the gap between the quasi-1D FS and quasi-2D FS and put two dimers in the unit cell. However, since the difference between them is quite small (only 2 % of its value),¹³⁾ we consider its difference can be neglected and regard the minimum model as the lattice with one site in the unit cell.

For the reasons stated above we adopt the following Hubbard Hamiltonian

$$\mathcal{H} = -t \sum_{\langle i,j \rangle, \sigma} c_{i,\sigma}^\dagger c_{j,\sigma} - t' \sum_{\langle i,k \rangle, \sigma} c_{i,\sigma}^\dagger c_{k,\sigma} + U \sum_i n_{i,\uparrow} n_{i,\downarrow} + \mu \sum_\sigma n_{i,\sigma}, \quad (2.1)$$

where σ is spin indices, $\langle i, j \rangle$ indicates taking summation over nearest neighbor sites and $\langle i, k \rangle$ over next nearest sites only in one direction as in Fig. 1. μ is the chemical potential which is determined so as to fix the electron number to 1 per site. The noninteracting energy

dispersion is;

$$\epsilon_{\mathbf{k}} = -2t(\cos k_x + \cos k_y) - 2t' \cos(k_x + k_y). \quad (2.2)$$

According to the quantum chemistry calculations,¹⁵⁾ we take $t'/t \simeq 0.7$ as the realistic value of κ -(ET)₂X. It should be noted that this lattice has strong frustration and can be called a nearly triangular lattice.

2.2 Green's function and self-energy

The non-interacting Green's function is the following;

$$G_0(\mathbf{k}, \epsilon_n) = \frac{1}{i\epsilon_n - (\epsilon_{\mathbf{k}} - \mu)}, \quad (2.3)$$

where $\epsilon_n = \pi T(2n + 1)$ (n is integer) is the fermion-Matsubara frequency. The diagrams of the normal self-energy are shown up to the third order of interaction in Fig. 2 (the Hartree term is included in the shift of chemical potential).

EPS File fig2.ps not found

Fig. 2. The diagrams of the normal self-energy up to the third order. The solid and dashed lines correspond to the bare Green's function and the interaction, respectively.

The analytic form of the normal self-energy is given by

$$\begin{aligned} \Sigma_n(\mathbf{k}, \epsilon_n) = & \frac{T}{N} \sum_{\mathbf{k}', n'} [U^2 \chi_0(\mathbf{k} - \mathbf{k}', \epsilon_n - \epsilon_{n'}) \\ & + U^3 \chi_0^2(\mathbf{k} - \mathbf{k}', \epsilon_n - \epsilon_{n'}) \\ & + U^3 \phi_0^2(\mathbf{k} + \mathbf{k}', \epsilon_n + \epsilon_{n'})] G_0(\mathbf{k}', \epsilon_{n'}). \end{aligned} \quad (2.4)$$

In this equation χ_0 and ϕ_0 are represented as

$$\chi_0(\mathbf{q}, \omega_m) = -\frac{T}{N} \sum_{\mathbf{k}, n} G_0(\mathbf{k}, \epsilon_n) G_0(\mathbf{q} + \mathbf{k}, \omega_m + \epsilon_n), \quad (2.5)$$

$$\phi_0(\mathbf{q}, \omega_m) = -\frac{T}{N} \sum_{\mathbf{k}, n} G_0(\mathbf{k}, \epsilon_n) G_0(\mathbf{q} - \mathbf{k}, \omega_m - \epsilon_n). \quad (2.6)$$

The anomalous self-energy can be divided into two parts, one of which is included in FLEX, and the other is not included in FLEX, i.e. the vertex correction. These diagrams are shown in Fig. 3 and Fig. 4, respectively.

Analytically these diagrams are written as following equations.

$$\Sigma_a(\mathbf{k}, \epsilon_n) = \Sigma_{\text{RPA}}(\mathbf{k}, \epsilon_n) + \Sigma_{\text{vert}}(\mathbf{k}, \epsilon_n), \quad (2.7)$$

EPS File fig3.ps not found

Fig. 3. The diagrams of the RPA parts(which are included in FLEX) of the anomalous self-energy up to the third order.

EPS File fig4.ps not found

Fig. 4. The diagrams of the vertex correction parts(which are not included in FLEX) of the anomalous self-energy up to the third order.

where $k = (\mathbf{k}, \epsilon_n)$.

2.3 The particle number

The particle number is 1.0 per site in the real system. However, in our perturbation scheme, there is a discrepancy between the particle number based on the bare Green's function(which is denoted by n_0) and that based on the dressed Green's function(which is denoted by n) in our perturbation scheme. The bare susceptibility($\chi_0(\mathbf{q}, \omega_m)$) plays an important role in the calculation of T_c , that is, it determines the magnitude and the spatial and temporal variation of the interaction between the particles. To incorporate the nature of half-filling, we put $n_0 = 1$, and require the number conservation between n_0 and n . To satisfy this requirement we introduce the shift of chemical potential $\delta\mu$, which is included in the following dressed Green's function;

$$G(\mathbf{k}, \epsilon_n) = \frac{1}{i\epsilon_n - (\epsilon_{\mathbf{k}} - \mu - \delta\mu + \Sigma_n(\mathbf{k}, \epsilon_n))}, \quad (2.10)$$

and the particle number is given by

$$n = 2 \frac{T}{N} \sum_{\mathbf{k}, n} G(\mathbf{k}, \epsilon_n). \quad (2.11)$$

To satisfy $n = 1.0$ up to the third order of the interaction, expanding eq. (2.11) with regard to $\delta\mu - \Sigma_n(\mathbf{k}, \epsilon_n)$, and using $n_0 = 2 \sum_{\mathbf{k}, n} G_0(\mathbf{k}, \epsilon_n) = 1.0$, then we get

$$\delta\mu = -\frac{\frac{T}{N} \sum_{\mathbf{k}, n} G_0^2(\mathbf{k}, \epsilon_n) \Sigma_n(\mathbf{k}, \epsilon_n)}{\chi_0(\mathbf{0}, 0)}. \quad (2.12)$$

$$\Sigma_{\text{RPA}}(\mathbf{k}, \epsilon_n) = -\frac{T}{N} \sum_{k'} [U + U^2 \chi_0(k+k') + 2U^2 \chi_0^2(k+k')] F(k'), \quad (2.8)$$

$$\begin{aligned} \Sigma_{\text{vert}}(\mathbf{k}, \epsilon_n) &= -U^3 \frac{T^2}{N^2} \sum_{k', k_1} G_0(k') (\chi_0(k+k') - \phi_0(k+k')) G_0(k+k'-k_1) F(k_1) \\ &\quad -U^3 \frac{T^2}{N^2} \sum_{k', k_1} G_0(k') (\chi_0(-k+k') - \phi_0(-k+k')) G_0(-k+k'-k_1) F(k_1), \end{aligned} \quad (2.9)$$

2.4 Éliashberg equation

For the calculation of T_c , the Dyson-Gor'kov equation is linearized as

$$F(\mathbf{k}, \epsilon_n) = |G(\mathbf{k}, \epsilon_n)|^2 \Sigma_a(\mathbf{k}, \epsilon_n). \quad (2.13)$$

Then the Éliashberg equation is given by

When the eigen value of this equation is 1, the system is considered to be superconducting i.e. $T = T_c$. We don't assume the symmetry of the Cooper pair in calculating T_c , which differs from Hotta,⁷⁾ but calculating T_c and determining the symmetry are performed simultaneously.

§3. Calculated Results

3.1 Details of the numerical calculation

We take the transfer integral t as the unit of the energy and put $t = 1$. From the quantum chemistry calculations,¹⁵⁾ $t \simeq 70 \sim 80$ meV, then T_c which is experimentally measured around 10K, is normalized to $T_c = 0.011$. The full bandwidth is from 8 to 9 when the value of t' varies from 0 to 1.

To solve the Éliashberg equation we have to calculate the summations over the momentum and the frequency space. Since all these summations are in the convolution forms, we can carry out these by using the algorithm of the Fast Fourier Transformation. For the frequency, irrespective of the temperature, we take 1024 Matsubara frequencies, which makes the frequency cut-off comparable to the bandwidth at $T \simeq 0.0020$. On the other hand, for the momentum space, in order to avoid the finite size effect at low temperatures,¹⁶⁾ we set points as fine as possible and divide the first Brillouin zone into 128×128 meshes.

3.2 Transition temperature

We calculate T_c by solving the Éliashberg equation (2.14). The gap function shows the node at $k_x = k_y$ and $k_x = -k_y$ and changes the sign across the node in all approximations and for all parameters, namely

$$\Sigma_a(\mathbf{k}, \epsilon_n) \propto \cos k_x - \cos k_y. \quad (3.1)$$

The symmetry of Cooper pair is $d_{x^2-y^2}$. The U -dependence of T_c is shown in Fig. 5.

In this figure, we show also the results obtained by FLEX calculation and that for only the RPA-like dia-

EPS File fig5.ps not found

Fig. 5. The calculated T_c . TOPT(RPA-only) in this figure means that only RPA-like diagrams of anomalous self-energies up to third order are included.(All normal self-energies are included up to the third order.) The diagonal transfer $t' = 0.7$. The unit of energy is the transfer t .

grams(of anomalous self-energies) included in TOPT, in addition to TOPT calculation for comparison. This results indicate that for larger U higher T_c are obtained commonly for all approximations of calculations. This is quite natural for our perturbation scheme and corresponds well to the experimental results which are measured by applying the pressure;¹⁷⁾ the pressure increases the bandwidth W and then U/W is reduced.

We can see the differences between TOPT and FLEX in Fig. 5; T_c calculated by FLEX is higher than TOPT for moderate values of U . This is because RPA-like diagrams are included up to higher order in FLEX, and the spin-fluctuation is largely enhanced. This reasoning is supported by comparison between TOPT and TOPT(RPA-only); the RPA-like diagrams of anomalous self-energies(eq. (2.8)) are responsible for attractive interaction, while the vertex corrections(eq. (2.9), this term is not included in FLEX as noted above) are responsible for repulsive interaction and then have the effect of lowering T_c (This was firstly pointed out by Hotta.⁷⁾). Therefore it can be said that the mechanism based on TOPT is the spin fluctuation induced one. The another difference between the results of TOPT and FLEX is their U -dependences. The rate of increase of T_c as U is varied in FLEX is slightly smaller than that of TOPT. This is probably due to the fact that the damping rate in FLEX is large because it is largely enhanced by the RPA diagrams, as well as the attractive interaction is enhanced.

There are many quantum chemistry calculations as mentioned above¹⁵⁾ and the obtained values for the transfer integral t' are roughly from 0.5 to 0.8, but it is difficult to know the real value of the transfer integral. Therefore it is meaningful to study the t' -dependence of T_c . The calculated results are shown in Fig. 6.

$$\begin{aligned}
 \Sigma_{\mathbf{a}}(k) = & -\frac{T}{N} \sum_{k'} [U + U^2 \chi_0(k+k') + 2U^2 \chi_0^2(k+k')] |G(k')|^2 \Sigma_{\mathbf{a}}(k') \\
 & -U^3 \frac{T^2}{N^2} \sum_{k', k_1} G_0(k') (\chi_0(k+k') - \phi_0(k+k')) G_0(k+k'-k_1) |G(k_1)|^2 \Sigma_{\mathbf{a}}(k_1) \\
 & -U^3 \frac{T^2}{N^2} \sum_{k', k_1} G_0(k') (\chi_0(-k+k') - \phi_0(-k+k')) G_0(-k+k'-k_1) |G(k_1)|^2 \Sigma_{\mathbf{a}}(k_1).
 \end{aligned} \tag{2.14}$$

EPS File fig6.ps not found

Fig. 6. The calculated t' -dependence of T_c in TOPT. The value of U is fixed to 6.50.

The obtained highest value is $T_c = 0.06400$ for $t' = 0.30$. For this value of $U = 6.5$, and within our numerical accuracy, T_c is not obtained for $t' \geq 0.8$. To obtain T_c for this region of t' , it is needed to increase U . At $t' = 0.00$, the Fermi surface is of perfect nesting and the bare susceptibility diverges. For this case we couldn't obtain the T_c .

The calculated results of the static bare susceptibility (eq. (2.5)) are shown in Fig. 7 for various values of t' .

EPS File fig7.ps not found

Fig. 7. The momentum dependence of the static bare susceptibility for various values of t' . These results are obtained for $T = 0.0500$.

For the typical value $t' = 0.70$, the susceptibility has the incommensurate peak around (π, π) and asymmetric peak around $(-\pi, \pi)$. This result indicates the $d_{x^2-y^2}$ symmetry of the gap function. This momentum dependence of the bare susceptibility is similar to the result of Kondo, *et al.*¹⁰⁾ obtained by FLEX. Therefore it can be said that both of the approaches which are TOPT and FLEX use the nesting property to acquire the spin fluctuation and the attractive interaction. Here, the t' -dependence has the following feature. When t' is decreased, the peaks at this momenta become sharper and then at $t' = 0.10$ the incommensurability and the asymmetry of the peaks disappear. These facts explain the results shown in Fig. 6, which generally shows higher T_c for smaller t' . Physically this corresponds to the fact that for smaller t' , the lattice is closer to the square lat-

tice and the antiferromagnetic fluctuation is larger due to reduced frustration. T_c at $t' = 0.1$ is lower than that of $t' = 0.3$ in spite of its sharper peak for $t' = 0.1$. This is because as t' decrease, the nesting property is enhanced and then the spectral density in the vicinity of the Fermi level moves to the two incoherent parts(i.e. which become the higher and the lower Hubbard bands in the Mott insulator). This transformation of the spectrum is shown in Fig. 8

EPS File fig8.ps not found

Fig. 8. The density of states as t' is varied, at $U = 6.50$ and $T = 0.06500$. The inset shows this figure focused near the Fermi level.

In order to see how the vertex corrections influence T_c when t' is varied, we also calculate T_c by including only RPA-like diagrams(Fig. 3) in anomalous self-energies, in other words, neglecting the vertex corrections. The results are shown in Fig. 9.

EPS File fig9.ps not found

Fig. 9. t' -dependences of T_c , calculated by including only RPA-like terms in anomalous self-energies(All normal self-energies up to the third order are included.), and by TOPT. The value of U is fixed to 6.50.

For a comparison with TOPT in the order of magnitude, we take the linear-log plot as is shown in the figure. For the case that only RPA-like anomalous self-energies are included, we can also see that for smaller t' , higher T_c is obtained for the same reason as the calculation by TOPT(Fig. 6). However, as t' is increased, the rate of decrease of T_c by TOPT (which includes the vertex corrections) is larger than TOPT(RPA-only). This property

of t' -dependence is clearly shown in Fig. 10.

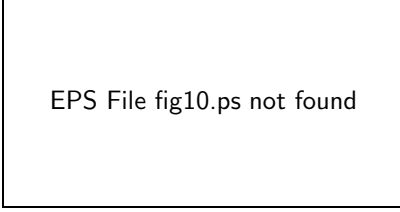


Fig. 10. t' -dependences of $|T_c - T_c^{\max}|/T_c^{\max}$, these values are calculated based on Fig. 9. Here, T_c^{\max} is the maximum value of T_c by each method(i.e. TOPT or TOPT(RPA-only)), when t' is varied. The value of U is fixed to 6.50.

From Fig. 9 and Fig. 10, we can clearly see that for larger t' , T_c is largely reduced by taking the vertex corrections. At $t' \simeq 0.3, 0.4$, the value of T_c by TOPT is half or one third of that by TOPT(RPA-only). This ratio is comparable to the high- T_c calculation by Hotta.⁷⁾ However, at $t' = 0.70$ corresponding to the real system, the value of T_c by TOPT is reduced by one order of magnitude compared with TOPT(RPA-only). This fact suggests that for large t' , i.e. when the frustration is large like our system, neglecting the vertex corrections is not a good approximation. Although the reason is not so simple from the complicated form of eq.(2.9), this property is probably due to the fact that the peaks of bare susceptibility are not so sharp for larger t' as is shown in Fig. 7. Because $\text{Re}\phi_0(\mathbf{q}, 0)$ doesn't have large t' -dependence as is shown in Fig. 11, $\chi_0(\mathbf{q}, 0) - \text{Re}\phi_0(\mathbf{q}, 0)$ has more remarkable peak around $(0, 0)$ for large t' as is shown in Fig. 12.

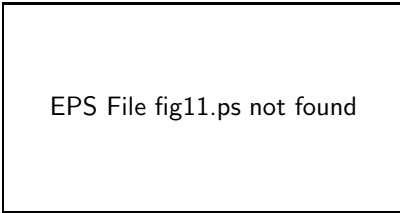


Fig. 11. The momentum dependence of $\text{Re}\phi_0(\mathbf{q}, 0)$ from eq. (2.6) for various values of t' . These results are obtained for $T = 0.0500$.

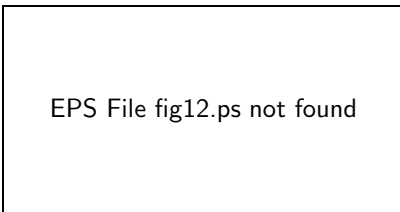


Fig. 12. The momentum dependence of $\chi_0(\mathbf{q}, 0) - \text{Re}\phi_0(\mathbf{q}, 0)$ for various values of t' . These results are obtained for $T = 0.0500$.

From Fig. 12, it is seen that for small t' , the peak around (π, π) makes the whole structure featureless.

However, for large t' , the strong frustration makes the peak around $(0, 0)$ remarkable. Therefore the vertex corrections affect the gap function more repulsively for the d-wave symmetry at large t' from eq. (2.9). In other words, they suppress the antiferromagnetic spin-fluctuation. Although within the third order perturbation, it can be said that the vertex corrections have a crucial effect on the calculation of T_c for strongly frustrated systems.

3.3 Density of states and self-energy

The density of states(DOS) is given by

$$\rho(\omega) = -\frac{1}{\pi} \sum_{\mathbf{k}} \text{Im}G(\mathbf{k}, \omega). \quad (3.2)$$

We calculate $\text{Im}G(\mathbf{k}, \omega)$ from eq. (2.10) by using the Padé approximation.¹⁸⁾ The U -dependence of DOS is shown in Fig. 13.

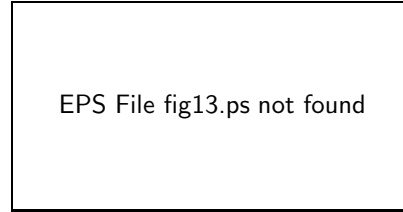


Fig. 13. DOS at $T = 0.01500$, $t' = 0.70$ and various values of U as shown in the figure. The arrows indicate the incoherent peaks for each value of U .

From this figure we can see that the incoherent peaks, which are corresponding to the upper and the lower Hubbard peaks, grow as U increases.(The upper peak can be seen for small U , while the lower peak can be seen only for large U . This tendency reflects the original asymmetric structure of DOS.) This is the expected behavior for our perturbation scheme because for larger U we approach the Mott-insulator phase, and coincides with the investigation on the infinite dimensions.¹⁹⁾ This behavior cannot be obtained within FLEX as is shown in Fig. 14, although U is very large and the system is expected to be close to the Mott insulator.

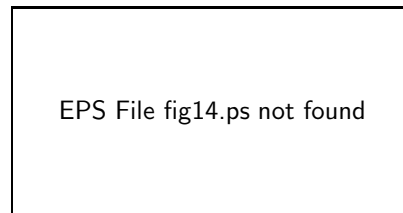


Fig. 14. DOS calculated by FLEX at $T = 0.02000$, $t' = 0.70$ and various values of U as shown in the figure.

The origin is probably ascribed to the self-consistent requirement in FLEX. In addition to this we see the asymmetric structure of DOS as expected for the nearly triangular lattice in Fig. 13 (i.e. because of the particle-hole asymmetry.). There is the coherence quasi-particle

peaks near the Fermi levels for all values of U , and we cannot obtain the pseudogap behavior within our model and approximation.

The normal self-energy is obtained from eq. (2.4) by using Padé approximation.¹⁸⁾ The real part($\text{Re}\Sigma_n(\mathbf{k}, \omega)$) and the imaginary part($\text{Im}\Sigma_n(\mathbf{k}, \omega)$) of the self-energy at the Fermi momentum are shown in Fig. 15 and Fig. 16 respectively.

EPS File fig15.ps not found

Fig. 15. The real part of the normal self-energy at the Fermi momentum, at $T = 0.01500$, $t' = 0.70$ and various values of U as shown in the figure.

EPS File fig16.ps not found

Fig. 16. The imaginary part of the normal self-energy at the Fermi momentum, at $T = 0.01500$, $t' = 0.70$ and various values of U as shown in the figure

The ω -dependence of both parts near $\omega = 0$ are respectively given by $\text{Re}\Sigma_n(\mathbf{k}, \omega) \propto -\omega$ and $\text{Im}\Sigma_n(\mathbf{k}, \omega) \propto -\omega^2$. (The small dip of the imaginary part at $U = 7.0$ in Fig. 16, might be ascribed to the lack of accuracy of the Padé approximation.) This behavior is the expected one for the usual Fermi liquid, and is opposite to the result of Maly, *et al.*²⁰⁾ which shows in their research in high- T_c $\left. \frac{\partial \text{Re}\Sigma_n(\mathbf{k}, \omega)}{\partial \omega} \right|_{\omega=0} > 0$ and $\left. \frac{\partial^2 \text{Im}\Sigma_n(\mathbf{k}, \omega)}{\partial \omega^2} \right|_{\omega=0} > 0$ obtained by using t -matrix approximation, resulting in the appearance of the pseudogap behavior. Other points which should be noted in Fig. 15 and Fig. 16 are that, as U increases, the slope of $\text{Re}\Sigma_n(\mathbf{k}_F, \omega)$ at $\omega = 0$ becomes steeper and the coefficient of ω^2 for the imaginary part becomes bigger. This indicates that the mass and the damping rate of the quasi-particle become larger (physically this corresponds to the increase of the resistivity) as U increases because the mass enhancement factor is given by $1 - \left. \frac{\partial \text{Re}\Sigma_n(\mathbf{k}, \omega)}{\partial \omega} \right|_{\omega=0}$ and the damping rate is given by $-\text{Im}\Sigma_n(\mathbf{k}, \omega)$. These results are the typical Fermi liquid ones, and cannot show the anomalous behavior like the pseudogap.

§4. Summary and Discussion

In this paper we have calculated T_c for the simple effective model of κ -(ET)₂X by solving the Éliashberg

equation on the basis of TOPT, and have investigated the possible mechanism by the spin fluctuation on this superconductor. We have adopted the Hubbard model with a nearly triangler lattice in which one of these transfer integrals, $t' = 0.7$; we have taken U as a parameter corresponding to the experiment in which the pressure is applied, and fixed the system to half-filling in agreement with the real compound. The obtained results roughly agree with the experiment in the high pressure region in its U -dependence and values.

The results obtained here show that the superconductivity in this organic conductor possibly arises from the same mechanism, by which we mean the antiferromagnetic spin fluctuation induced superconductivity, as that of the cuprate system, since both of them are connected by changing a single parameter t' .

We have also compared the results obtained by TOPT and FLEX. For the moderate value U , T_c of FLEX is higher than that of TOPT. This is because FLEX involves the higher order spin fluctuation in spite of its large damping rate. However, from our perturbative aspect, because of the offset between large attractive interaction and large damping which are both given by RPA-like diagrams, the appropriate values of T_c are obtained by FLEX. Therefore it should be noted that whether so large enhancement is physical one or not is a future problem. Concerning this point, we have shown in Fig. 5 and Fig. 9 that the vertex corrections reduce T_c by one order of magnitude. Up to the third order terms, it is found that the vertex corrections reduce T_c of strongly frustrated systems like our system, more seriously than that of not so frustrated systems like high- T_c , although it cannot be said generally beyond the third order from our scheme. This fact suggests that the calculations of T_c which include only the RPA-like terms are questionable and should be carefully performed with the vertex corrections

To investigate to what extent this scheme is effective, we study DOS and the normal self-energy. The obtained behaviors of both quantities are the expected ones for the Fermi liquid near the Mott-insulating phase. Especially the upper and the lower Hubbard bands in DOS are obtained in our perturbation scheme, while they are not obtained by FLEX. From this behavior of DOS, it is doubtful that the physical quantities obtained by FLEX have the nature of being near the Mott-insulating phase. It can be said that one of the elements which improve FLEX is possibly to take this property into account.

From the results of DOS and the self-energy, this perturbation approach is valid in the conventional metallic phase in the phase diagram of McKenzie.²¹⁾ However the (pseudo-)spin gap which is one of the most interesting properties in the strongly correlated electron system, is not reproduced in our scheme.

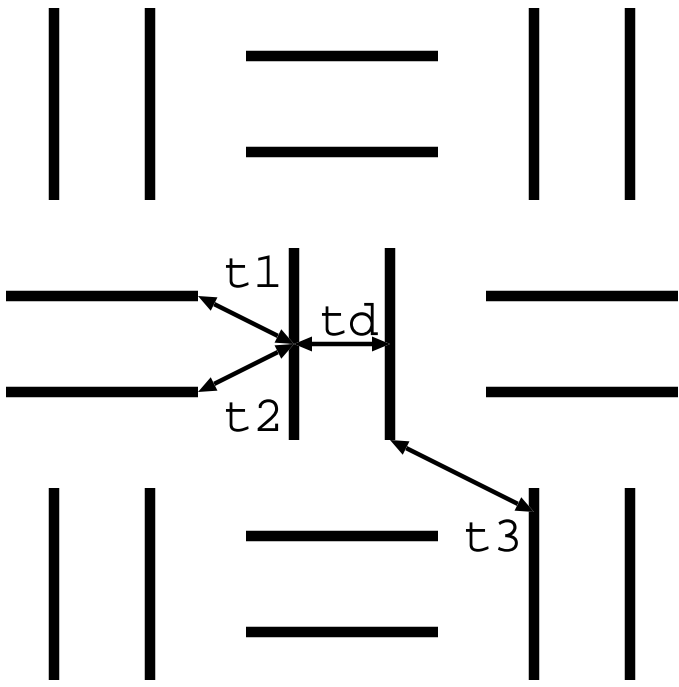
From the analytic property in the power series expansion of U for the Fermi liquid, we cannot derive this unconventional property by using the present method like TOPT or FLEX. There must be the crossover which shows the breakdown of the Fermi liquid at a certain value of U as is already found in experiments. It has not been known yet that this breakdown is caused by the su-

perconducting fluctuation^{20),22)} or the antiferromagnetic long(or short)-range order^{5),23)} or other mechanism. It is important to decide the critical term which characterizes the crossover and its effective region of the temperature and the magnitude of correlation. This is the problem to be solved to understand this compound and the nature of the non-Fermi liquid adjacent to the Fermi liquid.

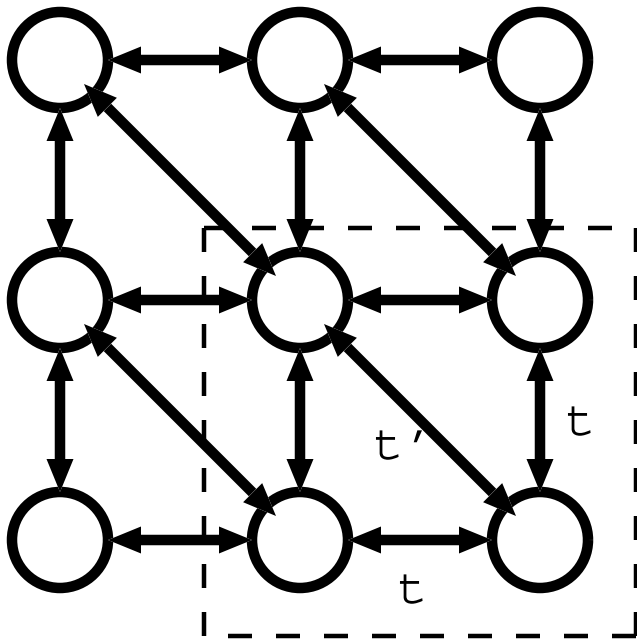
Acknowledgment

Numerical computation in this work was carried out at the Yukawa Institute Computer Facility.

-
- [1] K. Kanoda: *Physica C* **282-287** (1997) 299. , *Hyperfine Interactions* **104** (1997) 235.
 - [2] H. Mayaffre, P. Wzietek, D. Jérôme, C. Lenoir and P. Batail: *Phys. Rev. Lett.* **75** (1995) 4122. ; S. M. De Soto, C. P. Slichter, A. M. Kini, H. H. Wang, U. Geiser and J. M. Williams: *Phys. Rev. B* **52** (1995) 10364. ; K. Kanoda, K. Miyagawa, A. Kawamoto and Y. Nakazawa: *Phys. Rev. B* **54** (1996) 76. ; Y. Nakazawa and K. Kanoda: *Phys. Rev. B* **55** (1997) R8670.
 - [3] P. W. Anderson: *Science* **235** (1987) 1196.
 - [4] T. Moriya, Y. Takahashi and K. Ueda: *J. Phys. Soc. Jpn.* **59** (1990) 2905.; T. Moriya and K. Ueda: *J. Phys. Soc. Jpn.* **63** (1994) 1871.
 - [5] D. Pines: *Z. Phys. B* **103** (1997) 129. and references therein.
 - [6] H. Shimahara and S. Takada: *J. Phys. Soc. Jpn.* **57** (1988) 1044.; H. Shimahara: *ibid.* **58** (1989) 1735.
 - [7] T. Hotta: *J. Phys. Soc. Jpn.* **63** (1994) 4126.
 - [8] N. E. Bickers, D. J. Scalapino and S. R. White: *Phys. Rev. Lett.* **62** (1989) 961. ; N. E. Bickers and D. J. Scalapino: *Ann. Phys. (N. Y.)* **193** (1989) 206.
 - [9] J. Schmalian: *Phys. Rev. Lett.* **81** (1998) 4232.
 - [10] H. Kino and H. Kontani: *J. Phys. Soc. Jpn.* **67** (1998) 3691.; H. Kondo and T. Moriya: *ibid.* **67** (1998) 3695.
 - [11] H. Mayaffre, P. Wzietek, C. Lenoir, D. Jérôme and P. Batail: *Europhys. Lett.* **28** (1994) 205. ; A. Kawamoto, K. Miyagawa, Y. Nakazawa and K. Kanoda: *Phys. Rev. Lett.* **74** (1995) 3455.
 - [12] K. Oshima, T. Mori, H. Inokuchi, H. Urayama, H. Yamochi and G. Saito: *Phys. Rev. B* **38** (1988) 938.
 - [13] J. Caulfield, W. Lubczynski, F. L. Pratt, J. Singleton, D. Y. K. Ko, W. Hayes, M. Kurmoo and P. Day: *J. Phys. Condens. Matter* **6** (1994) 2911.
 - [14] H. Kino and H. Fukuyama: *J. Phys. Soc. Jpn.* **64** (1995) 2726.; *ibid.* **65** (1996) 2158.
 - [15] T. Komatsu, N. Matsukawa, T. Inoue and G. Saito: *J. Phys. Soc. Jpn.* **65** (1996) 1340. ; A. Fortunelli and A. Painelli: *J. Chem. Phys.* **106** (1997) 8051 ; M. Rahal, D. Chasseau, J. Gaultier, L. Ducasse, M. Kurmoo and P. Day: *Acta Cryst. B* **53** (1997) 159.
 - [16] J. W. Serene and D. W. Hess: *Phys. Rev. B* **44** (1991) 3391.
 - [17] Yu. V. Sushko, V. A. Bondarenko, R. A. Petrosov, N. D. Kushch, E. B. Yagubskii, M. A. Tanatar and V. S. Yefanov: *Physica C* **185-189** (1991) 2681. ; J. E. Schirber, D. L. Overmyer, K. D. Carlson, J. M. Williams, A. M. Kini, H. Hau Wang, H. A. Charlier, B. J. Love, D. M. Watkins and G. A. Yaconi: *Phys. Rev. B* **44** (1991) 4666.
 - [18] R. W. Haymaker and L. Schlessinger: in *The Padé approximant in Theoretical Physics*, G. A. Baker, Jr. and J. L. Gammel, eds. (Academic Press, New York, 1970) Chap. 11. ; H. J. Vidberg and J. W. Serene: *J. Low Temp. Phys.* **29** (1977) 179.
 - [19] X. Y. Zhan, M. J. Rozenberg and G. Kotliar: *Phys. Rev. Lett.* **70** (1993) 1666.
 - [20] J. Maly, B. Jankó and K. Levin: *cond-mat/9805018*.
 - [21] R. H. McKenzie: *Science* **278** (1997) 820.
 - [22] V. J. Emery and S. A. Kivelson: *Nature* **374** (1995) 434.
 - [23] A. V. Chubukov and D. K. Morr: *Phys. Rep.* **288** (1997) 355.



(a)



(b)

